Noname manuscript No.
(will be inserted by the editor)

Symptotics: A Framework for Estimating the Scalability of Real-World Wireless Networks

Ram Ramanathan · Ertugrul Ciftcioglu · Abhishek Samanta · Rahul Urgaonkar · Tom La Porta

Received: date / Accepted: date

Abstract We present a framework for non-asymptotic analysis of real-world multi-hop wireless networks that captures protocol overhead, congestion bottlenecks, traffic heterogeneity and other real-world concerns. The framework introduces the concept of *symptotic* [1] *scalability* to determine the number of nodes to which a network scales, and a metric called *change impact value* (CIV) for comparing the impact of underlying system parameters on network scalability. A key idea is to divide analysis into generic and specific parts connected via a *signature* – a set of governing parameters of a network scenario – such that analyzing a new network scenario reduces mainly to identifying its signature.

Using this framework, we present the first closed-form symptotic scalability expressions for line, grid, clique, randomized grid and mobile topologies. We model both TDMA and 802.11, as well as unicast and broadcast traffic. We compare the analysis with discrete event simulations and show that the model provides sufficiently accurate estimates of scalability. We show how our impact analysis methodology can be used to progressively tune network features to meet a scaling requirement. We uncover several new insights, for instance, on the limited impact of reducing routing overhead, the differential nature of flooding traffic, and the effect real-world mobility on scalability.

Keywords Multi-hop Wireless Network · Network Design · Scalability · Performance Model

Research was sponsored by the Army Research Laboratory and was accomplished under Cooperative Agreement Number W911NF-09-2-0053. The views and conclusions contained in this document are those of the authors and should not be interpreted as representing the official policies, either expressed or implied, of the Army Research Laboratory or the U.S. Government. The U.S. Government is authorized to reproduce & distribute reprints for Government purposes notwithstanding copyright notation here on..

Ram Ramanathan
Raytheon BBN Technologies
E-mail: ramanath@bbn.com

Ertugrul Ciftcioglu, Tom La Porta
Pennsylvania State University
E-mail: (enc118 | tlp)@psu.edu

Abhishek Samanta
Northeastern University
E-mail: asamanta@ccs.neu.edu

Rahul Urgaonkar
IBM Research
E-mail: rurgaon@us.ibm.com

[1] The word "symptotic" is not part of the English lexicon. We borrow from the commentary of Euclid's Elements by Proclus [1] ".. some are asymptotic, namely, those which however far extended never meet, and others that do intersect are *symptotic*.."

1 Introduction

Consider the following problem: a multi-hop wireless network running OLSR [2] routing over 802.11 radios needs to be deployed in a roughly regular structure (Manhattan grid). Each node needs a VoIP stream to another node (say randomly chosen) and is active 20% of the time. Roughly how many nodes N can one deploy?

Such a question, with straightforward variations, may arise in diverse situations: deploying an instant infrastructure wireless network after a disaster, a community wireless mesh network in a rural area, a military network, a sensor network, etc. Often, the answer does not need to be precise, but quick, and for a wide range of parameter combinations. Currently the only reasonable way available to answer such questions is to construct a simulation model and iterate over different values of N to find the upper bound. Not only does this take a prohibitively long time when N is large, but also requires re-running over again to answer follow up questions: what if we used a faster radio, or used different protocols, or a different encoding for VoIP is used? What if it is a different topology or a different traffic pattern? Last,

but not least, simulations do not provide insight into the relationships between parameters, or into which parameters dominate.

Analytical modeling appears a natural fit. However, much of the analytical research thus far has been along *asymptotic* lines (e.g [3–6]). While these have provided tremendous insight in the limiting case, asymptotic scalability has limited applicability to finite real-world networks. A network may be asymptotically unscalable, yet scale comfortably to the requisite number of nodes in a given deployment. Further, such work does not consider control protocols, congestion bottleneck effects, and the multiplicity of traffic types. Therefore, the results of these works (e.g. [3]) cannot be straightforwardly applied to modeling real-world networks where these considerations are of paramount importance. Finally, while there exist some analyses of specific protocols (such as 802.11), an analytical model of a *network scenario* – a combination of the topology, protocols, node and traffic attributes – as a *whole* is what we need.

In this paper, we present *symptotics* – a framework for approximate non-asymptotic closed-form modeling of wireless network performance. Unlike asymptotic analysis that typically characterizes a network in binary terms ("does it scale or not"), symptotics seeks to provide a qualified answer ("how many nodes does it scale to"). To this end, the framework introduces the concept of *symptotic scalability*. It accommodates real-world concerns including protocol overhead effects, congestion bottlenecks and multiple traffic types such as unicast and broadcast. It provides a unified approach to analytically model a suite of network scenarios without re-working the analysis for each, and a systematic way of determining the impact of changing a scenario parameter on performance. Finally, it provides closed-form models which, although harder than numerical solutions, give us insight into relationships between parameters and enable sensitivity (impact) analysis.

Our thesis is that the performance of a network scenario is dominated by a few major factors, and by focusing on those, one can obtain closed-form models with reasonable accuracy while avoiding complexity. Specifically, we divide the model into two parts – a) a generic equation for a class of network scenarios that captures the performance in terms of a set of major factors termed the *signature* of the scenario; b) instantiation of this equation using the specific signature of the given network scenario to derive a non-asymptotic (symptotic) closed-form expression for this network scenario. Thus, analyzing a new scenario requires doing only part (b) rather than re-working from scratch. Using the Sage mathematical software [7], we have been able to analyze new scenarios or different parameter values very quickly.

We illustrate the application of our framework by first deriving approximate symptotic scalability expressions for three static, regular topologies (line, grid, clique). For each we derive expressions with two MAC protocols (TDMA, 802.11) and two traffic types (unicast, broadcast), giving 12 models in all. A comparison with simulation results shows that despite their simplicity, our models are adequate for the rough estimations motivated at the beginning of this section, and lend support to our thesis that reasonable accuracy can be obtained with simple, approximate models. We then apply our framework to more complex topologies such as random and mobile networks, and derive closed form symptotic expressions for those scenarios.

A valuable part of the symptotic framework is a rigorous and uniform approach to *impact analysis*, that is, which parameters affect the overall system performance the most. As part of the framework, we introduce the concept of *change impact value* (CIV) to quantify the impact of domain parameters in a uniform way. By comparing the CIVs, we can tell, for example, if halving the offered load is better or worse for scalability than halving the routing overhead. We show how one can use CIV's to swiftly tune a network's features to meet a scaling requirement and estimate which parameter is critical in which conditions.

Using symptotic analysis, we have uncovered several new insights on multi-hop network performance that are difficult to discern using asymptotic analysis. We show that the impact of reducing routing overhead pales in comparison with that of equivalent changes in the radio rate or load (effected via compression techniques, for example) in typical scenarios. Load balancing, a relatively neglected approach, on the other hand not only increases scalability but also increases the gains from reducing overhead. The scalability behavior under flooding (network-wide broadcast) traffic is markedly different from that under unicast traffic, for instance in its dependence on density and relative performance between a randomized and regular grid. Finally, we observe that the repeated traversal mobility pattern reduces scalability by over an order of magnitude for typical parameters.

The rest of the paper is organized as follows. We begin by discussing related work in section 2. Section 3 describes the symptotic framework, and the derivation of a "master template" equation. In section 4 we illustrate the use of our framework by analyzing static, regular network scenarios. In section 5 we compare the analytical model with simulation results for the same network scenarios using ns-2. In section 6 we illustrate how the framework can be extended beyond regular networks to random and mobile scenarios. Impact analysis is covered in section 7, after which we present some concluding remarks.

2 Related Work

The scalability of wireless networks has mostly been studied along asymptotic, and information-theoretic lines – [3,

4,8,6,5] are a representative sample. Such asymptotic analyses seek to determine the fundamental scaling law underlying a network in terms of the order-of-growth. In [3], often considered the seminal paper in this area, the authors show that the per-node transport capacity of arbitrary wireless networks grows as $\Theta(\frac{1}{\sqrt{n}})$ indicating asymptotic unscalability. In [4], random mobile networks are shown to scale as $\Theta(1)$, or in other words, asymptotically scalable assuming unlimited delay tolerance. Directional antennas are shown not to help in the asymptotic sense [8] whereas distributed MIMO [6] with some assumptions scales as $\Theta(1)$. In this body of work, the assessment of scalability is unqualified (e.g. "Network X does not scale"), whereas symptotics seeks a qualified assessment (e.g. "Network X with parameter set P scales to 1000 nodes"). Further, these works do not consider real-world aspects such as protocol overhead, bottlenecks, or traffic heterogeneity.

There has been some recent work non-asymptotic analysis [9–13], but these have focused on specific aspects such as spectrum sensing [10], latency issues [11,13], or gateway effects in mesh networks [12], and none of them consider effect of routing control protocols or mobility.

Analysis of specific protocols, especially 802.11, has received a lot of attention [14–16], and specific properties of OLSR [2] have been analyzed [17]. Regular networks have been analyzed in [18,19] for stability and capacity, albeit with specific focus on capacity regions [18] or impact of buffer sizes [19]. Related work for our impact analysis methodology is sensitivity analysis, which has been studied using simulation [20], and analytically using Automated Differentiation techniques in [21]. Some of these works consider real-world aspects, but focus on specific protocols or issues (e.g. delay) rather than the system as a whole, and are not focused on scalability. They also do not target closed-form expressions, which we seek due to their ability to provide insights and assist in impact analysis. Our prior works [22, 23] adopt a similar analytical approach but not in depth, and do not consider randomized or mobile networks.

This paper is the first system-level (vice individual protocols), non-asymptotic, closed-form analytical model of real-world multi-hop, possibly mobile networks that considers control protocol effects at multiple layers and non-gateway congestion bottlenecks, and accommodates impact analysis.

3 The Symptotic Framework

The fundamental entity for analysis in our framework is a *network scenario*, which we define as a particular instantiation of the 4-tuple: network topology (e.g. grid, random), traffic type (e.g unicast, broadcast), node attributes (e.g. rate, number of transceivers), and control mechanisms (e.g. 802.11, OLSR).

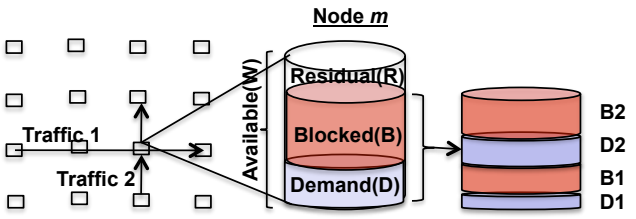

Fig. 1 The different components of capacity occupation at a representative node in the network.

Consider a representative node m in the network, along with its immediate neighborhood, as shown in Figure 1. We begin with a few definitions. The *available capacity* $W(m)$ indicates the amount of data that can be handled by m. The *demanded capacity* $D\ (m)$ denotes the amount of data load at m as a result of the offered traffic flows. We assume there are multiple classes or *types* of flows (e.g. web access, video etc), each of which can be one of network-wide broadcast ("flooding") or unicast (with uniform random source destination pairs). We assume that all flows of a given type have the same load profile in terms of packet rate and size. Note that we do *not* assume that all traffic is the same – different flow types can have different rates and packet sizes. The *blocked capacity* $B\ (m)$ denotes the capacity that is unusable by node m (for example, due to contention). The *residual capacity* $R(m)$ is the difference $W(m)$ - $D\ (m)$ - $B\ (m)$.

Both D and B may have components stemming from several flow types, each of which may have a different "cast" (unicast, broadcast) and/or a different "scope" (e.g., a one hop "Hello" vs. a network wide broadcast). Data, MAC control, network control, network management control etc., each have a different combination of cast and scope and are modeled as a different component of D and B . Thus, there are (the same) T traffic components at each node, each component j ($1 \leq j \leq T$) offers a different kind and amount of load on the network, and D and B are the sum of different components j. Thus, we have,

$$R(m) = W(m) - \sum_j D_j(m) - \sum_j B_j(m) \tag{1}$$

We note that, unlike most previous formulations that only consider one type of traffic (typically unicast with uniformly random source-destination pairs), we allow an arbitrary number of traffic flows each with a different profile and data rate. Since control and data traffic can be thought of as different profiles based on scope and cast, equation 1 captures not only data but also network control such as routing updates, thereby capturing overhead effects in our framework.

For sufficiently large networks with the kinds of topologies and random traffic that we consider in this paper (see section 3.1), the average traffic demand on neighbors of a node *m* in steady state is *approximately* the same as on m.

Note that we do *not* assume that *all* nodes in the network have the same, or even approximately the same load. Thus,

$$B_j(m) = \Gamma_j(m) \cdot D_j(m) \quad (2)$$

where $\Gamma_j(m)$ is the number of nodes in the neighborhood of m that either cause interference to, or in some other way cause m to defer when they are active.

We term Γ_j the *contention factor* for component j. The contention factor $\Gamma_j(m)$ depends on the topology around m, on the medium access control protocol in use, and the kind of transmission (e.g. unicast or broadcast), which in turn depends on the flow type of j. The contention factor is related to the spatial reuse achieved in a wireless network. The higher the contention factor, the lower is the spatial reuse.

Thus, from equations 1 and 2, we have

$$R(m) = W(m) - \sum_j (1 + \Gamma_j(m)) D_j(m) \quad (3)$$

Now consider $D_j(m)$. This is the contribution to m's demanded capacity from component j. Let L_j denote the offered load for a given component j. The contribution to $D_j(m)$ is the traffic sourced by m plus the traffic from other sources relayed by m. We call the latter (the relayed traffic) the *transit factor* of j, and denote it by Υ_j . For example, in a 5 node line network with each node flooding one packet each, 4 packets are relayed by the central node, and so its transit factor is 4. A beacon signal sent periodically by a node has a transit factor of 0 since it is not relayed. The expected demanded capacity is then $D_j(m) = L_j \cdot (1 + \Upsilon_j(m))$.

Finally, many medium access control schemes (e.g. CSMA/CA) have non-trivial *inefficiency*, that is, the effective rate is lower than the actual rate. Thus, the actual capacity available for multi-access communications is a fraction of W. Denoting MAC efficiency by η, and based on the above discussion, we rewrite equation 3 as

$$R(m) = \eta W(m) - \sum_j (1 + \Gamma_j(m)) L_j (1 + \Upsilon_j(m)) \quad (4)$$

We note that the equation 4 captures, in a unified way, both control and data flows each of which can be unicast or broadcast, the differences factored in terms of the contention and transit factors. Using equation 4, we now consider the definition of symptotic scalability and the generation of a "master template" for symptotic analysis.

3.1 Symptotic Scalability

As motivated in section 1, we seek non-asymptotic scalability, that is, to provide an answer to a question such as "to how many nodes will my network scale"? We begin by observing that such a question only makes sense for *expandable* network scenarios, that is, those that have a "scale agnostic" specification that allows one to create a network scenario at any scale. Examples of expandable network topologies include *regular* topologies such as line, ring, grid etc., as well as *irregular* stationary topologies based on some probabilistic model (e.g random unit-disk graphs, scale-free networks etc.), and mobile scenarios that have an expandable mobility model (e.g. the random waypoint model).

An arbitrary network with a specific set of nodes and a specific set of links between them is not expandable because there is no "rule" to generate higher-sized versions. Thus, the question "to how many nodes will a network scale" is well formed only for expandable networks, and not for arbitrary networks. We emphasize that our use of expandable networks is a necessary outcome of the question, and not an *assumption* that we are making. A similar differentiation can be made with respect to traffic as well. On the other hand, note that computing the *throughput capacity* of a given network is a reasonable proposition for arbitrary (non-expandable) networks.

We consider the class of expandable networks for which the residual capacity monotonically decreases as the size N increases. This class clearly includes regular networks with uniform traffic model. It also includes irregular expandable networks averaged over multiple instances, although a *particular* random network of size N may happen to have a higher residual capacity than a particular random network of size $N-1$. An example of a network scenario not in this class is when the set of nodes sourcing traffic is constant (say 1). Network scenarios not in this class are arguably asymptotically scalable and so are not of interest for symptotics.

For expandable networks, there is a point at which the monotonically decreasing residual capacity transitions from positive to negative. This is the maximum number of nodes supportable, or the "symptotic" scalability. We formalize this notion below. First, consider static networks. Let $R_N(m)$ denote the residual capacity of node m in a mobile network scenario with N nodes.

Definition 1 The *symptotic scalability* of a static network scenario is the number of nodes X such that for all $N \leq X$, and for all nodes m, $R_N(m) \geq 0$, and for all $N > X$, there exists a node m_b such that $R_N(m_b) < 0$.

We call m_b a *bottleneck node*. As the network size is increased, the bottleneck node is the node at which the residual capacity first becomes negative, and the size at which this happens is the symptotic scalability. When the resid-

ual capacity is positive, the bottleneck node is rate-stable, that is, the input rate is less than the service rate. A network scenario may have multiple bottlenecks, that is, nodes with equally lowest residual capacity, in which case m_b is any one of them.

We now consider mobile networks. We model mobile networks as a time-series of static network snapshots. Each snapshot is independent of the other, that is, there are no carryovers of queues from one snapshot to the next. This is a reasonable assumption in practice as typically the time scales for traffic dynamics are much smaller than those for topology changes. Each snapshot may be treated as a static network per definition 1 and assessed for symptotic scalability. We define the symptotic scalability of a mobile network scenario as the maximum number of nodes such that the residual capacity is positive for all nodes in *every* snapshot t. Formally, let $R_N(m,t)$ denote the residual capacity of node m at time snapshot t in a mobile network scenario with N nodes. Then,

Definition 2 The *symptotic scalability* of a mobile network scenario is the number of nodes X such that for all $N \leq X$, and for all nodes m, and all time snapshots t, $R_N(m,t) \geq 0$, and for all $N > X$, there exists a node m_b at time snapshot t_b such that $R_N(m_b,t_b) < 0$.

We call t_b a *bottleneck time*. A network scenario may have multiple bottleneck times, that is, snapshots with equally lowest residual capacity for some bottleneck node, in which case t_b is any one of them.

We note that definitions above are not based on throughput, and therefore inability to send traffic due to lack of routes does not impact it. Rather, what is relevant is if traffic is able to be sent, at what size the residual capacity will be zero. Thus, for instance, the symptotic scalability of a network with k disconnected cliques each of size m with $N = km$ is infinite as long as traffic within each clique does not zero-out the residual capacity.

We note that in this definition, a mobile network below the symptotic scalability size exhibits positive residual capacity at every node and always. This definition is closer in spirit to the "delay limited capacity" (see [24,25] for example) than the "ergodic capacity" of [3]. Alternate definitions are possible where it is not permissible for residual capacity to go below zero at some time snapshot and come back to positive thereafter, and those that consider transient queues. We have chosen the more conservative definition because in practice network operators rarely want to deploy networks so close to the edge that even having temporary overloads is acceptable.

Setting $R(m_b) = 0$ per definition 1, and dropping the reference to m_b and t_b with the notion that hereinafter it is implicit, we have from equation 4

$$\eta W = \sum_j (1 + \Gamma_j) L_j \cdot (1 + \Upsilon_j) \tag{5}$$

where η is the efficiency, $W$is the available capacity (radio rate), Γ_j is the contention factor for traffic type j, L_j is the average offered (sourced) load (in bps) per node for type j, and Υ_j is the transit factor for traffic j.

Equation 5 may be considered the "master template" that we further instantiate on a per-scenario basis. This requires us to further expand the above parameters to generate the expression characterizing the performance for that system. Specifically, the contention factor Γ_j and the transit factor Υ_j for each j play a critical role in the performance, and will be referred to as the *signature* of the system. To estimate the performance of a given system, one simply has to identify the signature and plug it into the master template. For asymptotically unscalable[2] networks, the transit and/or the contention factors are a function of N and hence equation 5 is of the form $\eta W = f(N, L_j)$, which can then be solved for N. In section 4, we give several detailed examples of how to identify the signature of a network scenario and instantiate and solve the master template.

In contrast with previous works (e.g. those mentioned in section 2), equation 5 can capture a multiplicity of traffic types that a typical real-world system has. For instance, consider a network in which each node generates VoIP as well as web-browsing traffic, each with a different source rate and destination distribution, and additionally a network-wide "situational awareness" broadcast traffic. Each of these can be modeled with a separate signature (Γ_j , Υ_j). Further, control traffic is accommodated simply as yet another traffic type.

The Symptotics framework can be applied to derive expressions for either *throughput capacity* as a function of network size or *scalability* as a function of offered load. In this paper, we mostly focus on scalability for two reasons. First, as motivated in the introduction, we seek to provide answers to questions such as "to how many nodes will my networks scale"? Second, scalability is harder to determine using simulation as it involves iterating (searching) over several network instances for "saturation". That said, analyzing throughput capacity can be very useful as well, and our implementation of Symptotics in the Sage software [7] contains both sets of expressions.

[2] The typical multi-hop wireless network is asymptotically unscalable [3]. While our framework can accommodate asymptotically scalable networks as well, these are largely uninteresting from a symptotic viewpoint as the scalability is infinite nodes.

4 Static Regular Network Scenarios

In this section, we illustrate the application of the symptotic framework from section 3, in particular the master template equation 5, to simple static topologies, namely the *line*, *planar grid* (with each node having 4 neighbors), and *clique* (fully connected network). For each of these, we derive symptotic scalability expressions – *unicast* and *flooding* (network-wide broadcast) data flows, and two MAC protocols – *TDMA* (Time Division Multiple Access) and IEEE *802.11* DCF, for a total of 12 network scenarios.

We assume the use of proactive event-driven link-state based routing. Overhead consists of *Link-State Updates* (LSU) that are flooded upon change in link state as well as periodically, and beacons ("Hello") one-hop broadcasts. We assume the use of hop-count as the routing metric. We restrict ourselves to one type of data traffic, namely unicast, for simplicity. Thus, with reference to equation 5, $j = 3$. Thus, for the purposes of this section, the specific master equation we consider is

$$\eta W = (1 + \Gamma_d)L_d(1 + \Upsilon_d) + (1 + \Gamma_l\ )L_l(1 + \Upsilon_l) + (1 + \Gamma_h\ )L_h(1 + \Upsilon_h\ ) \quad (6)$$

where Γ_d, Γ_l and Γ_h denote the contention factors for data, LSUs and Hellos respectively, Υ_d, Υ_l, and Υ_h denote the transit factors for data, LSUs and Hellos respectively, and L_d, L_l and L_h denote the offered load per node for each traffic type respectively.

For network-wide broadcast (flooded) packets such as LSUs and flooded data, we assume a single broadcast transmission at the MAC layer by each node[3]. We assume the "protocol model" for interference [3] for contention factor modeling. While we recognize that the physical (SINR) model is a better reflection of radio characteristics, recent work [26] has shown that one can narrow the gap between the two models by appropriately setting the interference range.

We organize the rest of this section with the top level being the MAC protocol – TDMA and 802.11. For each, we illustrate the application of the symptotic framework by determining the contention and transit factors for each of Line, Grid and Clique topologies, and for unicast and broadcast traffic. For each specific case, the analysis has the following steps: a) identify the bottleneck, if relevant; b) determine the signature; c) substitute the signatures into the master template to obtain the expression; d) solve for N. The last step is sometimes laborious to do by hand and so we have used the Sage mathematical and symbol manipulation software [7].

[3] An alternate model/assumption would be multiple unicast transmissions at the link layer, and can also be easily analyzed with our framework if necessary.

4.1 TDMA-based Regular Networks

We consider a spatial-reuse TDMA model with node scheduling, also referred to a broadcast scheduling [27] which is an abstraction of real-world TDMA implementations, for example [28]. We use an abstraction rather than a specific TDMA protocol for wider applicability and to avoid results from being tied to peculiarities of specific designs. That is, time is slotted and slots are grouped into repeating frames. Every node is assigned a slot in a frame in which it is allowed to transmit and its neighbors receive. Thus, nodes that are neighbors or share a common neighbor should be assigned different slots. The goal of a TDMA protocol is to perform conflict-free assignment using the least possible number of slots. Our model captures the control overhead – an integral part of any real TDMA implementation – for its operation by means of an additional "control slot" at the beginning of each frame. We assume that the control and data slots are of the same length. The control slot may be further subdivided into mini-slots for control purposes in a protocol-specific way.

The signature set for TDMA-based networks is given in Table 1. The first three columns contain the contention factor, and the second three contain the transit factor. The last column is the result of substituting the corresponding contention and transit factors into equation 6 and solving for N. To understand the table, it suffices to explain how we got the contention and transit factors, which we do below for each row.

We note that since Hello packets are only transmitted one hop, the transit factor Υ_h is zero for all topologies. Similarly, a flooded packet is transmitted by every other node in line and grid and hence Υ_l is $N - 1$, whereas it is not re-transmitted in clique so Υ_l for clique is 0. Thus, we only consider the first 4 columns of Table 1 below. Further, for flooding traffic including LSUs, all nodes are equal bottlenecks and therefore the residual capacity of interest is at the bottleneck node for unicast. Without loss of generality we assume an odd number of nodes (for line) and rows and columns (for grid), and therefore the center node as bottleneck.

4.1.1 Line Networks

A line network can be node scheduled using 3 slots, for example, using slot numbers 1, 2, and 3 repeating from left to right on the line. Thus, a typical node has to defer for nodes transmitting in slots other than its own and the control slot, and thus the contention factor is 3 for both link-layer unicast and broadcast. Since all traffic uses one of these modes, all of the contention factors are 3.

Consider the transit factor (TF). The TF for flooded data is clearly the same as that of LSUs, and therefore, $\Upsilon_d = N-1$.

	Contention Factor			Transit Factor			Scalability Expression
	Γ_d	Γ_l	Γ_h	Υ_d	Υ_l	Υ_h	N =
Line Flooding	3	3	3	N-1	N-1	0	$\frac{W\eta - 4\,L_h}{4\,(L_d + L_l)}$
Line Unicast	3	3	3	$\frac{(N-1)^2}{2(N-2)}$	N-1	0	$\frac{W\eta - 2\,L_d - 4\,L_h}{2\,(L_d + 2\,L_l)}$
Grid Flooding	5	5	5	N-1	N-1	0	$\frac{W\eta - 6\,L_h}{6\,(L_d + L_l)}$
Grid Unicast Non LB	5	5	5	$0.4(1 + \frac{2}{\sqrt{N}})(N^{\frac{3}{4}} + 4N^{\frac{1}{4}})$	N-1	0	See below
Grid Unicast LB	5	5	5	$\sqrt{N}$	N-1	0	$\frac{\left(3\,L_d - \sqrt{6\,L_l W\eta - 36\,(L_d + L_h)L_l + 9\,L_d^2}\right)^2}{36\,L_l^2}$
Clique Flooding	N-1	N-1	N-1	0	0	0	$\frac{W\eta}{L_d + L_h + L_l}$
Clique Unicast	N-1	N-1	N-1	0	0	0	$\frac{W\eta}{L_d + L_h + L_l}$

Table 1 Signature set and symptotic scalability expressions for regular networks using TDMA.

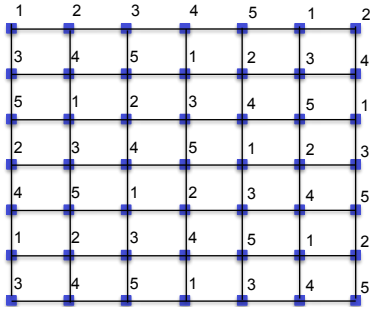

Fig. 2 An example conflict-free slot assignment for a 7x7 grid using 5 slots.

For the TF of unicast data, we need to compute the expected number of paths that go through b. The probability that a given node routes through b is the probability that the destination lies on the "other side" of b, that is, $p(B) = \frac{(N-1)/2}{N-2}$. Thus, the expected number of paths is $p(B) \cdot (N-1)$ as shown.

4.1.2 Grid Networks

We consider a grid network of N = m x m nodes. Such a grid network can be scheduled using 5 slots using a straightforward assignment scheme as shown with an example for a 7x7 grid in Figure 2. This is tight, since there clearly is a 2-hop clique of 5 nodes each of which would need a different color. Thus, our model captures a TDMA protocol that uses 5 slots to color a grid in addition to the control slot.

Consider the contention factor. With node scheduling, the node of interest has to defer for nodes transmitting in 4 slots other than its own, plus the control slot, that is, equivalent of 5 nodes. Thus, the contention factor is 5 in both cases for all traffic.

Consider the transit factor (TF). Clearly, the TF of flooded data is $N-1$ similar to the line. For the TF of unicast data, we need to compute the expected number of paths through the center node b. In the appendix, we have derived an approximate formula for the number of expected paths through the center as $0.4(1 + \frac{2}{\sqrt{N}})(N^{\frac{3}{4}} + 4N^{\frac{1}{4}})$.

Due to the complex radicals in the transit factor, we could derive a closed form for N only using an approximation of the transit factor, and even this is much too long to display in this or any paper. While this does not hamper us from generating numbers for plots using numerical techniques in mathematical software, it does make it cumbersome to work with for insights. Therefore, we have also provided a much simpler closed-form expression using a lower bound for the expected number of paths through the center as $\sqrt{N}$, derived in [19]. This lower bound also happens to correspond to the case when routing does the best possible load balancing of its traffic [19]. Thus, there are two rows – LB (Load Balanced), and Non LB (Non Load Balanced) in Table 1. The Non LB assumes that traffic is forwarded along shortest paths, ties broken randomly. Note that this will result in uneven load and when the center node gets saturated, there may still be capacity at the "edges" of the grid. The LB assumes that the routing protocol balances the load, say using the "row first column next" approach in [19]. We shall use both the Non LB and LB models as appropriate in the ensuing sections.

4.1.3 Clique Networks

A clique or "complete" network is one in which all nodes are mutually adjacent. Given node scheduling, in both unicast and flooding, every packet is transmitted exactly once. Thus, the symptotics are identical for unicast and flooding. No node is a bottleneck, and so any reference node can be taken. Since every node needs a slot, the CF is clearly $N-1$ for all three traffic types. Also, since no packet is ever relayed, the transit factors are zero for all traffic types.

4.2 802.11 based Regular Networks

In this section, we develop symptotic expressions for Line, Grid and Clique networks with IEEE 802.11g DCF [29] as the underlying MAC protocol. We assume that link-level unicast transmission is always done via an RTS-CTS-DATA-ACK (RCDA) handshake, and MAC-level broadcast transmission consists simply of the DATA transmission.

The signature set for 802.11-based networks is given in Table 2. We note, however, that the transit behavior as well

	Contention Factor			Transit Factor			Scalability Expression
	Γ_d	Γ_l	Γ_h	Υ_d	Υ_l	Υ_h	N =
Line Flooding	2	2	2	N-1	N-1	0	$\frac{W\eta - 3\,L_h}{3\,(L_d+L_l)}$
Line Unicast	3	2	2	$\frac{(N-1)^2}{2(N-2)}$	N-1	0	$\frac{W\eta - 2\,L_d - 3\,L_h}{2\,L_d+3\,L_l}$
Grid Flooding	4	4	4	N-1	N-1	0	$\frac{W\eta - 5\,L_h}{5\,(L_d+L_l)}$
Grid Unicast Non LB	7	4	4	$0.4(1+\frac{2}{\sqrt{N}})(N^{\frac{3}{4}}+4N^{\frac{1}{4}})$	N-1	0	See below
Grid Unicast LB	7	4	4	$\sqrt{N}$	N-1	0	$\frac{\left(4\,L_d - \sqrt{5\,L_l W\eta - 5\,(8\,L_d + 5\,L_h)L_l + 16\,L_d^2}\right)^2}{25\,L_l^2}$
Clique Flooding	N-1	N-1	N-1	0	0	0	$\left(\frac{W\eta}{L_d+L_h+L_l}\right)^{0.93}$
Clique Unicast	N-1	N-1	N-1	0	0	0	$\left(\frac{W\eta}{L_d+L_h+L_l}\right)^{0.93}$

Table 2 Signature set and symptotic scalability expression for regular networks using 802.11.

as the bottleneck node is dependent on the topology and not on the MAC. Hence the transit factors are same as for the corresponding sections in the TDMA section (Table 1). Therefore, we will only discuss contention factors below, and refer the reader back to subsections in 4.1 for the explanation of the transit factor part of the signatures.

4.2.1 Line Networks

For MAC-layer unicast transmissions, without loss of generality, suppose bottleneck center b wants to send to node X. Clearly, due to RTS-CTS based deference behavior, b has to defer whenever its neighbors or neighbors of X are transmitting, and hence the contention factor is 3. For flooded data, as well as LSAs and Hellos, since MAC-layer broadcast is employed, RTS-CTS are not sent and so node b need only desist due to carrier sense which is when either of its neighbors are transmitting[4]. Hence CF is 2. It may appear strange that the broadcast contention factor is less than the unicast contention factor, but this merely models the way most real systems (e.g. [30]) work notwithstanding the penalty due to lack of reliability. We note that the actual throughput may be less due to lack of re-transmissions.

4.2.2 Grid Networks

Consider the contention factor for bottleneck center node b. For link-level unicast transmissions, without loss of generality, suppose b wants to send to node X. Since RTS-CTS is used, all nodes that receive the RTS or the CTS defer, and by reciprocity, the reference node has a contention factor of 7. For link-level broadcast transmissions (flooding data, LSUs and Hellos), there is no RTS-CTS, and the only deference is via carrier sense, and hence the contention factor is all neighbors, that is, 4.

[4] This is assuming the carrier sense range is same as transmission range. In reality, the carrier sense range depends on the radio. The assumptions is not critical in the context of the framework, that is, should the carrier sense range be two hops, one would merely replace the signature component to 4.

4.2.3 Clique Networks

The signature for clique networks under 802.11 is identical to that for TDMA since $N-1$ nodes cause deference by a given node.

However, there are two key factors that come into play with 802.11 that result in different symptotics. First, the overhead causes lower efficiency as discussed earlier. Second, as mentioned earlier, the backoff dynamics cause decreasing efficiency with increasing numbers of nodes. That is, as the probability of collisions and finding the channel busy increase with increasing number of nodes, the efficiency of 802.11 is lower and hence a clique network with 802.11 will scale to less nodes than with TDMA. While this is negligible for fixed degree regular networks such as line and grid, it cannot be ignored for clique as the degree is $O(N)$. This is more thoroughly analyzed in [31], where the efficiency is shown to decrease as $N^{-1.08}$. Using this, and the signature for 802.11 based clique is as given in the last two rows.

5 Validation

In this section we present results of ns-2 simulations of some of the scenarios analyzed in section 4. We instantiate the corresponding symptotic expressions given there and compare them with simulation results for the same set of parameter values (refer Table 3). For the link-state routing, we use header parameters from OLSR as a reasonable representative.

For the analytical results, the expressions in the last column of Tables 1 and 2 are used. The loads L_d, L_l and L_h are calculated based on the sourced packets per second (pps) for each of data (λ_d), LSU frequency (λ_l) and Hello frequency (λ_h) respectively, the payload size (we use 1000 bytes), and the network and MAC layer headers. For 802.11, the RTS, CTS, and ACK penalty is added when computing L_d. The header lengths and variables we use for the rest of this section are summarized in Table 3. The radio rate (W) and the offered flow rate (λ_d) are variable. The efficiency (η) is set to 1.0 to model idealized TDMA. In 802.11, the physical layer and MAC layer headers contribute to overhead that

results in efficiency $\eta < 1$. 802.11g uses OFDM and provides raw radio rates from 6 Mbps to 54 Mbps. The physical layer preamble is sent at the lowest rate and the contention window slots are fixed length. Thus, the efficiency reduces as the radio rate increases. Based on the derivation given in [15], the datarate (W) to efficiency (η) mappings we use are: (6 Mbps $\rightarrow$ 0.80), (12 Mbps $\rightarrow$ 0.70), (24 Mbps $\rightarrow$ 0.58), (54 Mbps $\rightarrow$ 0.40). For rates in between these numbers, the efficiency is linearly interpolated.

We now turn to the simulation set up. The TDMA protocol that we use is an extension of the TDMA model available in the ns-2 distribution. Specifically, we have extended it to a spatial reuse TDMA, that is, one that allows multiple nodes to transmit in the same slot. We then implemented a 3-slot assignment for line networks and a 5-slot assignment for mesh networks as described in section 4.1. The TDMA in ns-2 already models a control slot, which we have retained.

For 802.11, we have used the ns-2 model from an overhaul that significantly improves on the original model [32]. The key features include cumulative SINR computation, preamble and PLCP header processing and capture, and frame body capture. The MAC accurately models the basic IEEE 802.11 CSMA/CA mechanism, as required for credible simulation studies. The model implements models of four modulation schemes – BPSK, QPSK, 16-QAM, 64-QAM – with 1/2 coding rate for the first three and 3/4 for 64-QAM to provide four data rates: 6 Mbps, 12 Mbps, 24 Mbps, and 54 Mbps.

The physical layer propagation model is the *two-ray ground* model that is part of the WirelessPHYExt protocol for both TDMA and 802.11. The physical layer settings gives a transmission range of 450m. To create a line topology, we place nodes separated by a distance of slightly less than 450m such that only adjacent nodes are within range. Similarly, for a mesh, only nodes adjacent in 4 directions are within range. A clique is formed by ensuring that all nodes are within 450m of each other. The simulation duration is 30 seconds, sufficient for static networks.

We have studied the symptotic scalability N_{max} as a function of pps λ_d for each of the 12 network scenarios described in section 4. Per definition 1, at $N > N_{max}$ the residual capacity of at least one node is less than zero. At this point, the input rate on the node's transmit queue is more than the output, and the queue becomes unstable (that is, starts growing continuously). The ns-2 simulation system has a finite queue length – therefore, queue instability is detected as packets being dropped due to queue being full. In our simulations, the queue length is 50 packets, and we deem the network saturated if there are non-trivial queue drops, in particular, if there are 50 or more packets dropped.

Thus, we run simulations with increasing size N_i till we encounter two consecutive N_i and N_{i+1} such that there are no queue drops in N_i and there are non-trivial (> 50) queue drops in N_{i+1}. We then measure the symptotic scalability as the average of N_i and N_{i+1}. For example, if there are no queue drops for N=40, and non-trivial drops for N=50, the symptotic scalability is N=45. For the line and clique networks, the increment was 10 nodes and for a mesh, the side was incremented by 1 (i.e., the sizes were 16, 25, 36, 49 and so on).

Link State Routing	802.11
LSU : 52 bytes	RTS : 20 bytes
Hello : 48 bytes	CTS : 14 bytes
Net Hdr: 20 bytes	ACK : 28 bytes
LSU freq(λ_l) = 0.2 pps	MAC Hdr: 28 bytes
Hello freq(λ_h) = 1 pps	Payload size: 1 KB

Table 3 Protocol header sizes from [2,33].

We have considered alternate measures such as a sudden drop in throughput or increase in delay. The former is fairly unreliable especially for 802.11 networks where collisons cause loss. The latter correlates well with the queue drop measurement, but harder to objectively measure, and hence we have used queue drops as an indication of saturation.

Figures 3(a), (b), (c), (d) compare the symptotic scalability predicted by our model with simulation results. Since the simulations take a long time to run for larger sizes, we picked the radio rate and packets per second such that the y-axis maximum is not prohibitively large. Further, due to space constraints, we have only shown a subset of the plots, picking a subset such that each topology, MAC and traffic type is represented at least once.

Our results show that despite its simplicity and abstraction of details, the scalability predicted by our model matches that predicted by simulations fairly well, and adequately for practical purposes of estimating the rough order of magnitude as motivated in section 1.

The slight discrepancy between the analysis and simulation is due to several factors. First, the analysis is approximate by design, and in particular due to simplifications made in the course of the derivations (e.g. assuming $N - 1 \approx N$), the accuracy is lower for smaller N. On the other hand, we cannot compare using high N because simulations cannot scale to large sizes. Second, for unicast mesh results, we have assumed that routing picks randomly from amongst shortest paths, which may not be the case. Third, for CSMA results, the random processes are only captured in the aggregate. Finally, due to simulation running time constraints, the node step size granularity is high. In particular, in Figure 3(b) the derivation for mesh unicast in Appendix A is more approximate for small N and therefore we see higher discrepancy at lower N.

The simulation results attest to the fact that the approach taken and approximations and assumptions made do not excessively compromise accuracy. The differences seen are within reason, and the slopes parallel for the most part. Our simulation study gives us confidence that our model, despite

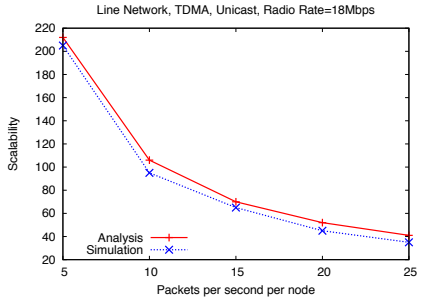

(a) TDMA, Line, Unicast, with 18 Mbps radio

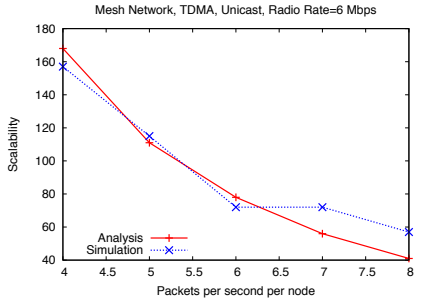

(b) TDMA, Mesh, Unicast, 6 Mbps radio

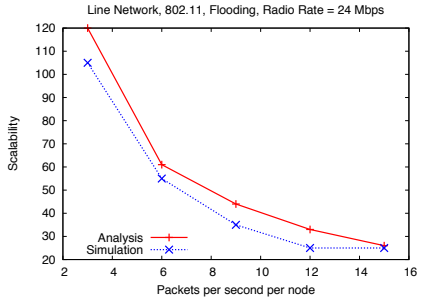

(c) 802.11, Line, Flooding, 24 Mbps radio

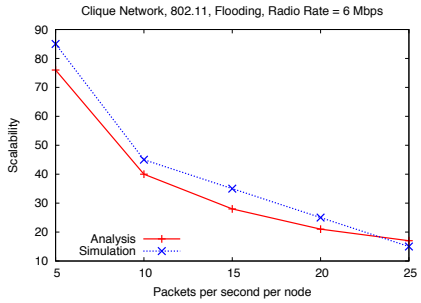

(d) 802.11, Clique, Unicast, 6 Mbps radio

Fig. 3 Comparison of analytical model with discrete-event simulation.

its simplicity, is adequate for rough order of magnitude scalability predictions. In the next two sections, with a validated model in hand, we turn our attention to more complicated and realistic scenarios, and to impact analysis.

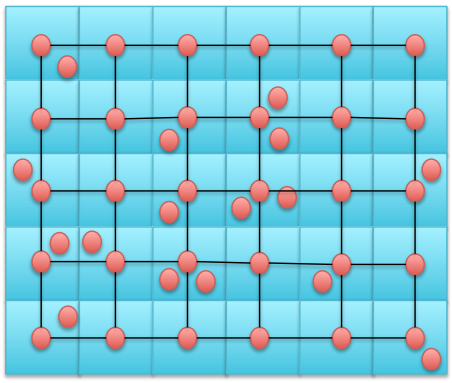

Fig. 4 Illustration of the Degree 4 Random Grid Network Model.

6 Other Scenarios: Randomness and Mobility

Thus far we have limited ourselves to topologies that are regular and static. In this section, we relax in a limited way both these constraints. In the next subsection we consider a random topology constrained by real-world connectivity considerations that we term a *randomized grid*, and in section 6.2, we consider a mobile scenario based on a real-world mobility model called *repeated traversal mobility*. Due to lack of space, we only present expressions with a subset of the MAC and traffic options considered earlier.

6.1 Grid-Based Random Networks

Real-world networks are seldom purely random, that is, with the nodes distributed uniformly randomly in space. Instead, we consider a class of random networks that we call "Grid Based Random Networks" which are formed as follows. First, we partition the network into M equal-sized disjoint "cells" and assume that there is at least one node per cell. We assume that nodes in adjacent cells are within communication range of each other. These two assumptions ensure that a network in this class is always a connected network, which is an important criterion for real-world networks. The remaining nodes are located uniformly at random over the cells. This is illustrated in Figure 4 where it is assumed that nodes in a cell can communicate with nodes in same cell and adjacent cells to the Left, Right, Top, and Bottom. Note that the grid-based random network is an expandable network as defined in section 3.1 and hence its symptotic scalability can be analyzed. A grid-based random network could model a community mesh network or a organized deployment of military squads, with a "cell" above modeling a community or a squad, respectively.

We assume there can be at most one concurrent transmission per cell and its adjacent cells. Define the node density ρ as the ratio of the total number of nodes N to the number of cells M ($N = M\rho$). Note that $\rho \geq 1$ since we assume at least one node per cell. The average node density in this network can be controlled by varying this parameter

ρ. Using the signature based analysis for the regular degree-4 grid based on M cells, we can now derive the symptotic scalability expressions this network. Given a ρ and a traffic demand, we define scalability of this random grid network as the maximum network size N that can support this demand for density ρ.

Suppose this network operates according to a spatial-reuse TDMA schedule per the assignment shown in Figure 2. Note that instead of "node scheduling", we have "cell scheduling". Assuming nodes within a cell divide the effective transmission rate equally, the contention factor (CF) and transmit factor (TF) under flooding and unicast for this network can be derived as follows. On average, a node has to contend with $5\rho - 1$ nodes in its own and neighboring cells. This plus the control slot yields a CF of $\Gamma_d = \Gamma_l = \Gamma_h = 5\rho$ for both unicast and broadcast. Next, consider the transit factor (TF). Similar to regular grid, the TF of Hellos is zero. Assuming that each node in a cell is equally likely to route a flooded packet generated by a node in another cell, we have $\Upsilon_d = M - 1$ for flooding while $\Upsilon_l = M - 1$ for both flooding and unicast traffic (where $M = N/\rho$). Finally, the TF for unicast data can be computed using the same procedure as regular grid but now based on cells, and is given by $\Upsilon_d = 0.4(1 + \frac{2}{\sqrt{M}})(M^{\frac{3}{4}} + 4M^{\frac{1}{4}})$ for non-load-balanced unicast and by $\Upsilon_d = \sqrt{M}$ for load balanced unicast.

Using these signatures in the master template, we get the following expression for scalability for flooding traffic.

$$N = -\frac{W\eta\rho - 5\,L_h\rho^2 - L_h\rho}{5\,(L_d + L_l)\rho + L_d + L_l} \tag{7}$$

For load-balanced unicast we get:

$$N = \frac{2\,L_l W\eta\rho - \sqrt{5\,\rho + 1}XL_d\rho - Y}{2\,(5\,L_l^2\rho + L_l^2)} \tag{8}$$

where

$$X = \sqrt{4\,L_l W\eta - 4\,(L_d + L_h)L_l - 5\,(4\,(L_d + L_h)L_l - L_d^2)\rho + L_d^2} \tag{9}$$

$$Y = 5\,(2\,(L_d + L_h)L_l - L_d^2)\rho^2 - (2\,(L_d + L_h)L_l - L_d^2)\rho \tag{10}$$

As with regular grid, the expression for non-load balanced are much too unwieldy to present. In what follows, we use the load balanced expressions for all numerical computations.

Figure 5 plots the scalability as derived above vs node density ρ for different values of the input traffic load for unicast and flooding respectively. It can be seen that while the scalability decreases with ρ for unicast, it initially increases and then appears to converge to a fixed value in case of flooding. These can be explained intuitively as follows. The scalability with increasing ρ (decreasing $M = N/\rho$) is governed by a tension between gains from reduced traffic and loss from increased contention. In the case of unicast, the gains from reduced traffic is $O(\sqrt{M})$ whereas loss from increased contention is $O(M)$, resulting in a decrease with increasing ρ[5]. For flooding on the other hand, the corresponding numbers are the same, namely, $O(M)$ and therefore the scalability is independent of ρ. The slight increase for smaller values of ρ is because we have assumed one control slot for TDMA irrespective of ρ and this overhead decreases with increasing ρ more discernibly for smaller values of ρ.

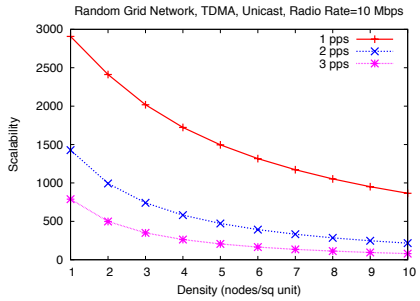

(a)

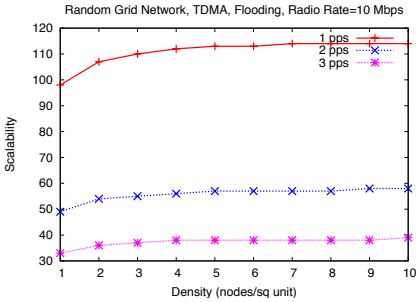

(b)

Fig. 5 Scalability vs density of randomized grid with TDMA for unicast (a) and flooding (b), each for three load levels 1, 2 and 3 pps per node.

An interesting question which we are now in a position to answer is: which is better, a regular grid or a random grid? Due to the way we construct the random grid with N depending on ρ, this is better answered by comparing the per-node capacity (throughput L_d) of each for varying N. Using symptotic analysis, we can derive the following expression for maximum per node load for unicast traffic for the random grid model:

$$L_d = \frac{W\eta - (5\,L_l\rho + L_l)M - 5\,L_h\rho - L_h}{(5\,\rho + 1)\sqrt{M} + 5\,\rho + 1} \tag{11}$$

Similarly, we can derive the following expression for maximum per node load for flooding for the random grid model:

[5] More precisely, $N \times \lambda \times O(\sqrt{\frac{N}{\rho}}) \leq N/\rho \implies N \leq O(\frac{1}{\lambda^2\rho})$

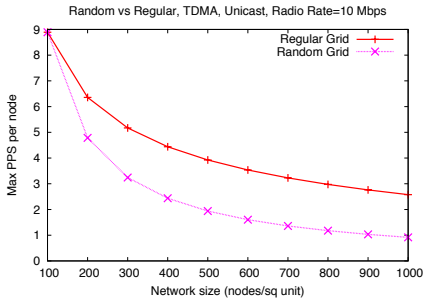

(a)

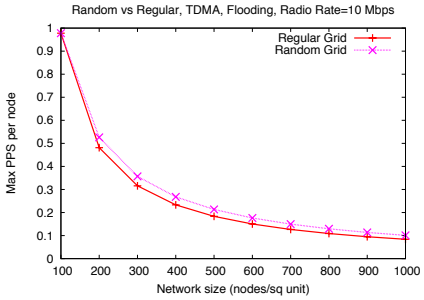

(b)

Fig. 6 Throughput vs size for random grid and regular grid for unicast (a) and flooding (b). Random grid does worse than regular grid with unicast, but interestingly does better with flooding.

$$L_d = \frac{W\eta - (5\,L_l\rho + L_l)M - 5\,L_h\rho - L_h}{(5\,\rho + 1)M} \tag{12}$$

Fig. 6 shows the comparison between random and regular grid. For the random grid model, we fix the number of cells $M = 100$ and then calculate the maximum feasible input rate per node for increasing values of ρ using the expression above. For regular degree-4 grid, we calculate the same quantity assuming a network of size $M\rho$, by using equation 6 but solving for L_d instead of for N as we did in section 4. Thus, we compare same-sized network in both cases, with size increasing on the X axis. It can be seen from Fig. 6 (a) that regular degree-4 grid outperforms random grid network for the same network size under unicast traffic. Intuitively, this also follows from the results of Gupta-Kumar [3] that suggest that for uniform unicast traffic, maximizing the number of concurrent transmissions by keeping transmission range as small as possible (while ensuring network connectivity) is optimal.

However, unlike unicast, we find that for flooding random grid slightly outperforms regular grid (figure 6(b)). Note that a pure asymptotic analysis would conclude that there is no performance gap in this case.

6.2 Mobile Networks

In this section, we use the symptotics framework to analyze a real-world mobility scenario often used in tactical networks (vice a synthetic one such as "random waypoint" which seldom exists in real-life). Specifically, we study the *repeated traversal*[34] mobility, as described in the next section.

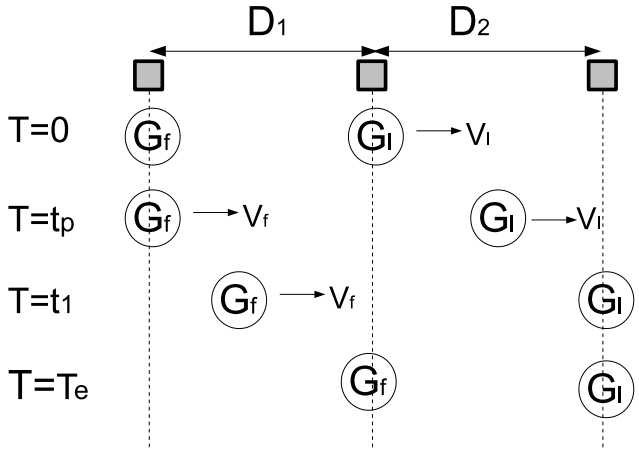

Fig. 7 Stages and connectivity of Repeated Traversal of convoy groups. G_f, G_l represent the following and leading groups respectively. G_l starts moving at time T=0, G_f at time T= t_p, G_l stops moving at time T = t_1.

The repeated traversal mobility model consists of two groups, called the *leading group*, and the *following group*. Initially, the groups are co-located. The leading group moves first and rests, after which the following group moves and joins the leading group. The process then repeats itself. Repeated traversal is prevalent in military troops through hostile terrain, where the leading squad of soldiers clears the terrain of threats before the following squad follows. The model is also applicable to civilian scenarios, notably disaster relief. An example of repeated traversal is depicted in Fig. 7.

Note that a network with repeated traversal mobility is an expandable network as defined in section 3.1 and hence its symptotic scalability can be analyzed. We study a specific case of the repeated traversal depicted in Fig.7 in which each group is arranged in a line, as might be the case when the groups are disaster relief convoys. We assume that the two groups are identical in terms of group size and node density. Specifically, distances between consecutive nodes are identical throughout each group. Moreover, we also assume that inter-group distances are significantly larger than intra-group distances, and the communication range of each node is such that it can reach all nodes in its group in one hop. Note that while the connectivity within each group is a "clique network", the fact that the nodes are in a line means that inter-group connectivity changes happen in a step-by-step manner than all at once. This is depicted in Figure 8.

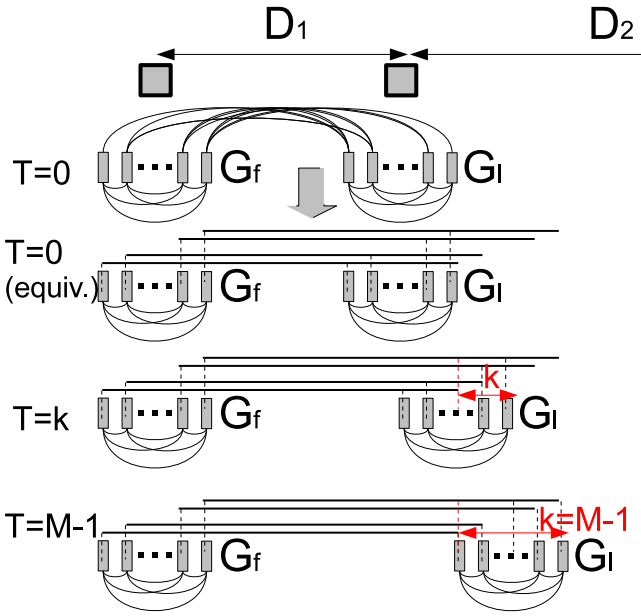

Fig. 8 Stages and connectivity of Repeated Traversal of convoy groups, leading group moving

Figure 8 also demonstrates the specific stages of different connectivity for the case when the leading group moves away from the following group, resulting in link breakages. For lack of space only T=0 to T=$M-1$ are shown. The pattern from then to T=$2M-1$, and the second part when the following group recovers the distance and links are created are similar in nature.

When both groups are in full communication range at the beginning of the movement, the overall network connectivity is a giant clique. As the leading group moves, after some time, some pairs of nodes from separate groups start to lose direct contact, leading to a different topology. During these stages, multi-hop relaying is required to communicate between nodes in different groups. Ultimately, when the groups are completely isolated, the network consists of two disjoint cliques.

The overall effect of mobility on symptotic scalability is two-fold: (i) Different stages of connectivity throughout movement results in different signatures $(\Gamma_j(t), \Upsilon_j(t))$ for each stage; and (ii) Link breakages and creations necessitate exchange of Link State Updates (LSU), increasing control overhead. The amount of LSU packets required depend on the number of link breakages or creations, hence potentially vary with the specific stage. Moreover, $(\Gamma_l(t), \Upsilon_l(t))$ also potentially depend on the stage number, since relaying options are changed.

Due to lack of space, we focus only on the simpler case of flooding traffic. We present the signatures of the network for the k^{th} stage number in Table 4, where stages increment with change of topology. The signatures of the stages

Mvmt Stage, k	$\Gamma_d(k)$	$\Gamma_l(k)$	$\Gamma_h(k)$	$\Upsilon_d(k)$	$\Upsilon_l(k)$
$k=0$	2M-1	2M-1	2M-1	0	0
$1 \leq k \leq$ M-1	2M-1	2M-1	2M-1	2k	2k
$M \leq k \leq$ 2M-1	2M-1	3M-1-k	3M-1-k	2M-1	2(2M-k)
$k=2M$	M-1	M-1	M-1	0	0

Table 4 Stages of Repeated Traversal and their signatures. $\Upsilon_h(k)$ is zero for all stages.

where the following group recovers the distance and connects again with the leading group is identical, only as a reverse sequence of the above.

For flooding, contention factors depend on number of neighbors as in static case and all traffic types have equal contention factors. However, transit factors vary for different traffic types. For data packets, every node creates packets. On the other hand, since the link-state routing is event-driven per our assumption, for LSU packets, only nodes which experience link breakages or formations send out control packets, hence LSU traffic generated each stage changes with movement stage, resulting in lower transit factors. Specifically, LSU traffic initially increases with stage number due to increasing number of link breakages and is maximized at stage $M-1$. Afterwards, the number of nodes from different groups that are in contact starts to reduce gradually, also reducing the number of link breakages and LSU traffic accordingly.

We now derive the symptotic scalability expression for repeated traversal. From equation 6 and Table 4, and noting that signatures are now a function of both the stage k and the group size M, we have

$$\begin{aligned}\eta W =&(1+\Gamma_d(M,k))L_d(1+\Upsilon_d(M,k))+(1+\Gamma_l(M,k))L_l \\ &\times(1+\Upsilon_l(M,k))+(1+\Gamma_h(M,k))L_d(1+\Upsilon_h(M,k)),\end{aligned} \tag{13}$$

for $\forall k$ such that $0 \leq k \leq 2M-1$, resulting in $2M$ equations for a given group size M.

We first fix M and investigate which stage k maximizes the RHS of (13), that is, determine the bottleneck node and stage. It is easily seen that the bottleneck stage is one of the intermediate stages between disconnected and fully connected network. Note that per definition 1 and related discussion thereof, the lack of traffic across the groups does not mean that the symptotic scalability is zero. Of these stages, it is clear that the contention factor for nodes that are closer to the other group is larger. Additionally, these nodes also have a higher transit factor, since they provide relaying for the farther nodes. As a result, at each intermediate stage, the two nodes from each group that are closest to the other group are the bottlenecks. In particular, we observe that the largest amount of loading occurs at stage $M-1$, which corresponds to the instance when only one member of each group still has contact with the other group as well.

Plugging in the signatures at $k = M - 1$, we have the following equation to characterize the scalable network size:

$$\eta W = 2ML_d 2M + 2ML_l 2M + 2ML_h \quad (14)$$

Since network size $N = 2M$, we have

$$\eta W = N^2 L_d + N^2 L_l + NL_h = N^2(L_d + L_l) + NL_h \quad (15)$$

Solving the quadratic equation for N and taking the only non-negative solutions, we have

$$N = \frac{\sqrt{L_h^2 + 4\eta W(L_d + L_l)} - L_h}{2(L_d + L_l)} \approx \sqrt{\frac{\eta W}{L_d + L_l}}. \quad (16)$$

for $L_d + L_l \gg L_h$.

How does this compare with static scenarios? Recall that the scalability of the closest static analogues, namely the line and the clique network was approximately $N \approx \frac{\eta W}{(L_d + L_l)}$ (refer section 4.1) which implies a linear increase in scalable size with radio rate. In contrast, we now have, from equation (16) a square root dependence for repeated traversal. In other words, to double the supported number of nodes, roughly the radio rate must be increased four times vice two times for static. On the other hand, equation (16) also reveals that the dependence between traffic load and scalable group size is roughly given by $N\alpha(L_d + L_l)^{-0.5}$, hence doubling the load only reduces scalable size by about 30 percent vice halving it for static.

We use the parameters from Table 3 in section 5, with radio rate W set to 10 Mbps for all plots where it is not varied and the flow rate per node set to 1 pps for all plots where it is not varied.

Figure 9 (a) plots the scalable network size as a function of radio rate W for both static and repeated traversal. First, we observe that repeated traversal reduces scalability by more than an order of magnitude. Specifically, for W = 2 Mbps, the scalability falls from 224 nodes for static to a mere 16 nodes for repeated traversal. Since contention factor for the static case is equal to $N - 1$, it is apparent that this decrease is due to the increase in transit factors Υ_d and Υ_l, in particular, at the bottleneck nodes at the edge in stage $M - 1$.

Finally, for fixed radio rate $W = 10Mbps$ we vary data traffic load λ_d in Figure 9(b). Also, as expected, the scalable group size does not reduce to half when load is doubled, but is rather larger, around the 70 percent as provisioned.

In sum, we have provided expressions for the scalability of repeated traversal for flooding traffic. We show that contrary to asymptotic results [4], mobility in certain scenarios *reduces* capacity and hence scalability in the symptotic regime. The main reason is the change in topology, and increased traffic in some specific nodes, which are the bottleneck nodes. Further, N varies as the square root of radio rate and the inverse square root of the load, which is asymptotically distinct from static where the relationship is linear.

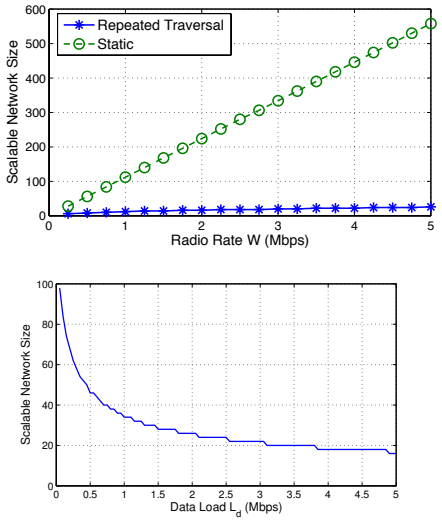

Fig. 9 Scalable network sizes for static and repeated traversal as a function of radio rate (a), scalable network size for repeated traversal as a function of data load (b).

7 Impact Analysis

In this section, we introduce the concept of *change impact value* for quantifying the impact of a particular parameter such as routing overhead, radio rate, or offered load on scalability, and illustrate how it can be used along with the symptotic models derived in the previous sections to drive design choices to meet a scaling requirement. We then study how their impact changes with nominal values of other network parameters.

7.1 Change Impact Value

In section 4, we derived several expressions of the form $N = f(X)$ where X= $(x_1, x_2, \ldots, x_n)$ is the parameter vector on which N depends. For example, in the symptotic scalability of a line network using TDMA and flooding, namely, $N = \frac{W\eta - 4\,L_h}{4\,(L_d + L_l)}$, X= W, η, L_h, L_d, L_l. These parameters define the scalability region for the network in question. The value of N for a specific network scenario obviously depends upon the values of the parameters.

A real-world system typically has a set of default or *nominal* parameters, for instance, as part of its initial configuration. Let V denote the *nominal instantiation* of the parameter vector X, with $(x_1 = v_1, x_2 = v_2, \ldots, x_n = v_n)$, where v_i is the nominal or default value of parameter x_i. Further, let $V_{x_j=k}$ represent that parameter x_j is *over-ridden* with value k in V, while all other parameters are as in the nominal instantiation.

Definition 3 The *Change Impact Value* of parameter x_j for a "change factor" α is $CIV(x_j, \alpha) = \frac{f(V_{x_j=\alpha \cdot v_j})}{f(V)}$.

In other words, $CIV(x_j, \alpha)$ is the factor change in scalability resulting from changing parameter x_j by α times its nominal value. For brevity, we shall often use "impact" to refer to the CIV.

For example, in the expression $N = W - C$, where V = (W = 100, C = 10), $CIV(W, 2)$ denotes the impact of doubling W on N and is the ratio between $2W - C$ and $W - C$ for nominal parameters V and is 190/90 = 2.11.

The CIV depends upon the choice of α for the particular parameter. Increasing a parameter may increase or decrease the function value, and vice versa. A parameter whose increase (decrease) increases (decreases) the function value is called *positively aligned*. A parameter whose increase (decrease) decreases (increases) the value is called *negatively aligned*. For example, the radio rate W is positively aligned and the routing overhead L_l is negatively aligned. To compare the impact uniformly, we shall specify the given value of α as greater than 1, and use $\alpha_p = \alpha$ for positively aligned parameters and $\alpha_p = 1/\alpha$ for negatively aligned parameters, where α_p is the change factor for parameter p. For instance, if we wanted to compare the impact of radio rate W and routing control packets per second λ_l for a change factor of 2, we would use α for W as 2 and α for λ_l as 0.5. This denotes, respectively, the impact of doubling the radio rate or halving the overhead, and provides an apple-to-apples comparison. The choice of α is left to the user, within reasonable limits. For instance, to determine the effect of an order-of-magnitude change rather than a factor-of-2, α could be set to 10. We only require that $\forall_{i,j}\ \alpha_i = \alpha_j$ or $\alpha_i = 1/\alpha_j$.

We note that the above is not equivalent to simply taking the differential coefficient and evaluating/instantiating it. To see this, consider two expressions $y = 1 + x$, and $y = 1000 + x$, and suppose the nominal value of x is 10. In both cases, *dy/dx* is 1, but the impact of doubling x is much lower for the second equation (CIV=1.01) than the first (CIV=1.91). This is because the constant (1000) in the second expression is much bigger relative to the nominal value of x in the second expression, and this is not captured adequately by the differential coefficient. The magnitude of nominal values play a crucial role in impact analysis for real-world networks, and our approach is tailored to accommodate that in the simplest possible manner.

7.2 Using CIV for Network Design

We begin by illustrating how impact analysis can be used to tune a system's features to meet a scalability requirement. Consider the following example scenario: A community mesh network has to be deployed in a very remote area to provide VoIP phones, mostly for a community of about 2000 houses to talk amongst themselves. The going-in architecture is to use OLSR over 802.11b radios (max rate 11 Mbps), a G.711 VoIP codec (174 kbps duplex, 132 pps, 160 byte packets including network- layer headers). For lack of any other information, traffic is assumed to be random unicast, and we assume a conservative active time of 20%.

Plugging these parameters into the symptotic equation in Table 2 for 802.11-based grid unicast (row 4), the scalability turns out to be only 116 nodes. To increase the scalability, we can either go to higher rate radios, a more efficient codec, or reduce routing overhead via a better routing protocol. We apply impact analysis from section 7.1, and compute the CIVs. Using $\alpha = 2$ for radio rate (W) and $\alpha = 0.5$ for source packets-per-second (λ_d) and routing overhead pps (λ_l)), we have the CIVs as: [6]

CIV(W) = 2.965; CIV(λ_d) = 2.811; CIV(λ_l) = 1.020

Thus, radio rate W and source rate λ_d are about equally dominant, providing approximately a 3x increase in scalability. However, source rate is more easily changed by using a better codec for very little tradeoff in clarity. Suppose we pick the G.723 codec (33 kbps duplex, 66 pps, 64 byte packets) instead with everything else remaining the same. This is factor of 5 lower in load and therefore we should expect it to scale much more than 2.811*116 = 326 nodes. Recalculating, the scalability is now 630 nodes, which is a vast improvement, but still well below the target 2000. Now, the CIVs are

CIV(W) = 2.588; CIV(λ_d) = 2.382; CIV(λ_l) = 1.000

Notice that depending upon the values of other nominal parameters, the impact of changing a parameter is different. In particular, the impact of changing W is now non-trivially higher. Given that we have already reduced λ_d, we turn to 802.11g radios with a maximum rate of 54 Mbps (a factor of $\tilde{5}$ improvement). With this, the scalability is about 2507 nodes which meets the requirement. Now the CIVs are

CIV(W) = 2.502; CIV(λ_d) = 2.231; CIV(λ_l) = 1.014

This suggests that if we could further double the radio rate, we might reach 2.5*2507 = 6250 nodes.

In all of the above, we notice that the CIV(λ_l), that is, the impact of routing load is negligible. While it is not surprising that radio rate and load are more impactful, we were surprised by the *magnitude* of the difference.

[6] Technology choices offer a range of factor-of improvements, and rather than pick different α's for each, we have simply picked the smallest integer factor, namely 2, for simplicity. The relative CIVs for $\alpha = 2$ should adequately capture the relative CIVs with other α's for our purposes.

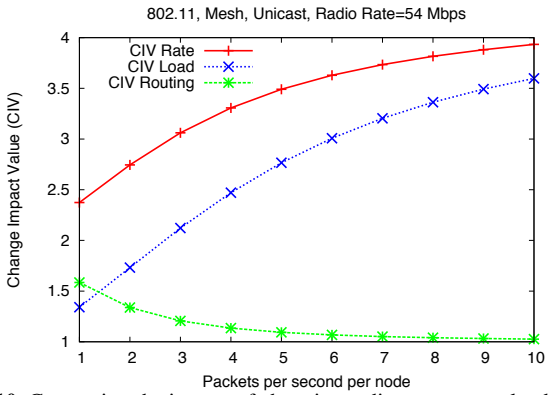

Fig. 10 Comparing the impact of changing radio rate, source load and overhead on scalability (higher CIV means more impactful)

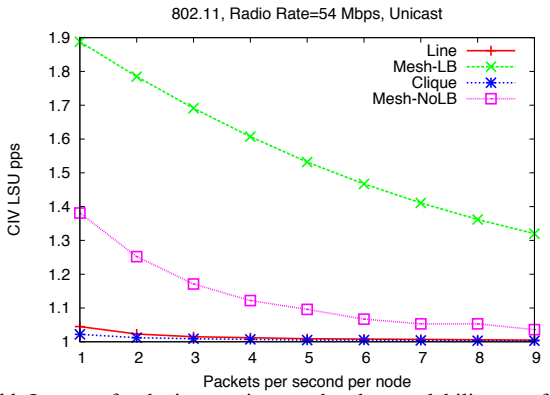

Fig. 11 Impact of reducing routing overhead on scalability as a function of load for line, clique and grid topologies, with load balanced and non-load-balanced versions (higher CIV means more impactful).

Given the amount of work that has gone into innovative techniques for reducing routing overhead in a multi-hop network, it would be helpful to know in what regimes, if any, routing overhead has a high impact on scalability. Accordingly, we present a study of the CIV as a function of various nominal parameters. We use a radio rate of 54 Mbps for the studies below.

Figure 10 shows the CIVs of radio rate, source load and overhead over a range of traffic loads. For a vast majority of this space, the impact of doubling radio rate or halving source load is vastly higher than halving overhead. The gap narrows at very low loads where reducing overhead becomes about equally important as halving offered load. This is because at low loads, the network scales to larger sizes in which routing overhead (which grows as $O(N)$ per node) occupies a larger fraction of the capacity. On the other hand, this is the regime in which scalability is at its highest, and one may not need the increase quite as much as at higher loads.

Figure 11 shows that the impact of overhead reduction is much higher for a regular grid than for line or clique, and higher when load balancing is used. This is because the lower the effective load on the bottleneck, higher is the fraction of LSUs, and consequently more impactful it is. Note that there are two benefits of load balancing (LB) – first, load balancing improves scalability. Instantiating the LB and non-LB expressions from section 4 for 54 Mbps, the improvement from LB (using the technique from [19]) can be as much as 5.2X at 5 pps. Over and above this, what is shown by impact analysis and Figure 11 is that having load balanced routing in turn increases the impact of reducing routing overhead, by about 40% at 5 pps.

We have gained a number of insights from impact analysis. First, as we have shown, computing the CIVs can assist in deciding which of several options provides the designer the most benefit for a given cost. Second, it appears that for most network scenarios the impact of radio rate and load on scalability is far higher than that of control overhead. Further, the absolute value of CIV for typical networks is close to 1, which means reducing it is largely ineffective for scalability[7]. Third, topologies with more opportunities to spread out traffic (e.g. grid with unicast) offer more gain from reducing overhead, reducing load or increasing radio rate. In particular, load balancing not only can significantly improve the scalability by itself, but also can significantly amplify the impact of routing protocol efficiency gains.

In the past, much emphasis has been placed on ideas for reducing routing overhead. In the big picture, though, improving the radio rate and codec technologies is much more impactful than overhead reduction in real-life wireless networks. On the other hand, load balancing has received scant attention relatively and holds the potential, in certain network scenarios for better impact.

8 Concluding Remarks

We have presented a novel framework for wireless network analysis that captures real-world considerations such as protocol overhead, traffic diversity, congestion bottlenecks etc. in a manner that asymptotic analysis does not. Our framework captures the system performance holistically in terms of its contention and transit factors that incorporate aspects at multiple layers of the stack. We have derived the symptotic scalability of 15 network scenarios, validated the model using simulations and presented a novel methodology for analyzing parameter impact.

Using symptotic analysis, we have presented several observations on the scalability of multi-hop wireless networks. We have shown that broadcast (flooding) traffic has different scalability behavior compared to unicast (e.g unlike unicast, flooding scalability does not decrease with density in a randomized grid). Also, in contrast to asymptotic results that

[7] Although our impact analysis has not considered mobile networks, we have used an LSU source rate of 0.2 LSUs per second which captures mobilities with link dyanmics of up to once every 5 seconds.

show that a random mobility pattern increases scalability even in the order sense, symptotic scalability of real-world patterns such as repeated traversal is significantly lower due to bottleneck effects. Further, our impact analysis shows that the effect of routing overhead reduction pales in comparison to equivalent increases in radio rate or decreases in load. Finally, load balancing – which has received much less attention than control overhead reduction – offers not only a significant scalability increase, but also makes the system more receptive to reducing control overhead. These and other such insights can help designers of MANETs, mesh and sensor networks.

There are several future research directions. First, as with any work in a new area, we have had to make some simplifying assumptions such as flow uniformity which can be relaxed. Another direction is to derive signatures for other traffic models (e.g. multicast, sink-based) with multiple data flows, other protocols (e.g. reactive) or node architectures (e.g multi-radio/multi-rate/cognitive network). A third interesting direction is to "triangulate" the symptotic scalability of a non-expandable arbitrary network by determining the scalability of a few representative expandable network models. The rudimentary impact analysis approach presented here, while useful, ought to be developed into a more sophisticated impact analysis theory. Finally, we would hope for a collaborative extension of this framework toward one that is more powerful, and that includes a growing "library" of signatures and the associated analyses.

[Shortest paths through degree-4 grid center]

A APPENDIX: Shortest paths through degree-4 grid center

We derive an approximate formula for the expected number of shortest paths between uniformly randomly selected nodes that go through the center of an m by m degree-4 grid containing $N = m^2$ nodes.

Consider the route from source s to a destination d. For the path from s to d to go through the center, they must clearly lie in the opposite quadrant inclusive of the nodes parallel and perpendicular to the center. Let $P_c(s,d)$ denote the probability that the path from s to d goes through the center, and $Q(d)$ denote the probability that d is in the opposite quadrant. Then the expected number of paths through the center is given by

$$E[P_c] = Q(d_q) \cdot P_c(s,d) \cdot (N-1) \tag{17}$$

Since we don't count the center node c and s,

$$Q(d) = \frac{(\frac{m+1}{2})^2 - 1}{m^2 - 2} \approx \frac{1}{4} + \frac{1}{2m} \tag{18}$$

$P_c(s,d)$ depends upon the exact location of s and d. Instead of iterating over all values of s and d (which gets very complicated very quickly), we approximate it by assuming the average to be equal to when s and d are in the centers of their respective quadrants, and denote

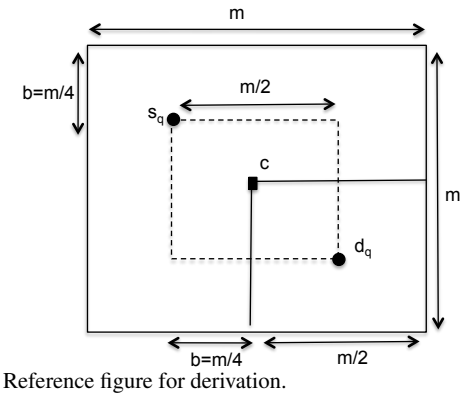

Fig. 12 Reference figure for derivation.

these nodes by s_q and d_q. Let $n(x,y)$ denote the number of shortest paths from x to y. Then

$$P_c(s,d) = P_c(s_q,d_q) = \frac{n(s_q,c) \cdot n(c,d_q)}{n(s_q,d_q)} \tag{19}$$

Given a square z by z grid, the number of shortest paths from one corner to another is $\binom{2z}{z}$[35]. Let $b = m/4$. Then, from figure 12 and the above, we have

$$P_c(s,d) = \frac{\binom{2b}{b}^2}{\binom{4b}{2b}} \tag{20}$$

The above is related to the concept of Catalan numbers [35]. The n^{th} Catalan number and an approximate formula thereof [36] are given by

$$C_n = \frac{1}{n+1} \cdot \binom{2n}{n} \approx \frac{4^n}{n^{1.5}\sqrt{\pi}} \tag{21}$$

Using eq. 21 in eq. 20, we have

$$P_c(s,d) = \frac{((b+1)C_b)^2}{(2b+1)C_{2b}} \approx \frac{0.8(b+1)}{b^{1.5}} \tag{22}$$

Re-substituting $b = m/4$ in the above, and using this and eq. 18 in 17, we have

$$\begin{aligned} E[P_c] &\approx (0.25 + \frac{1}{2m}) \cdot m^2 \cdot \frac{1.6(m+4)}{m^{1.5}} \\ &\approx 0.4(1 + \frac{2}{m})(m^{1.5} + 4m^{0.5}) \\ &\approx 0.4(1 + \frac{2}{\sqrt{N}})(N^{\frac{3}{4}} + 4N^{\frac{1}{4}}) \end{aligned}$$

References

1. G.R. Morrow, *Proclus: A commentary on the first book of Euclid's Elements* (Princeton University Press, 1970)
2. T. Clausen, P. Jacquet, in *IETF RFC 3626* (2003)
3. P. Gupta, P.R. Kumar, IEEE Transactions on Information Theory **46**, 388 (2000)
4. M. Grossglauser, D. Tse, IEEE/ACM Transactions on Networking **10**, 477 (2002)

5. M. Franceschetti, O. Dousse, D.N.C. Tse, P. Thiran, IEEE Trans. Inf. Theory **53**(3), 1009 (2007)
6. A. Ozgur, O. Leveque, D.N.C. Tse, IEEE Trans. Inf. Theory **53**, 3549 (2007)
7. W. Stein, et al., *Sage Mathematics Software (Version 4.7.2)*. The Sage Development Team (2011). `http://www.sagemath.org`
8. S. Yi, Y. Pei, S. Kalyanaraman, in *In 4th ACM MobiHoc* (2003), pp. 108–116
9. F. Ciucu, O. Hohlfeld, P. Hui, in *48th Annual Allerton Conference* (2010), pp. 662 –669
10. F. Penna, R. Garello, D. Figlioli, M. Spirito, in *Proc. CROWNCOM '09* (2009), pp. 1 –5
11. J. Liebeherr, A. Burchard, F. Ciucu, in *Proc. IEEE INFOCOM* (2010), pp. 1 –9
12. J. Jun, M. Sichitiu, Wireless Communications, IEEE **10**(5), 8 (2003)
13. N. Bisnik, A. Abouzeid, in *Proc. ICC '06*, vol. 1 (2006), vol. 1, pp. 403–408
14. G. Bianchi, Selected Areas in Communications, IEEE Journal on **18**(3), 535 (2000)
15. J. Jangeun, P. Peddabachagari, M. Sichitiu, in *Proc. of NCA 2003* (2003)
16. A. Jindal, K. Psounis, IEEE/ACM Trans. Netw. **17**, 1118 (2009)
17. D. Nguyen, P. Minet, in *Proc. AINAW '07*, vol. 2 (2007), vol. 2, pp. 887 –892
18. G. Mergen, L. Tong, IEEE Trans. Inf. Theory **51**(6), 1938 (2005)
19. G. Barrenetxea, B. Berefull-Lozano, M. Vetterli, IEEE/ACM Trans. Netw. **14**, 492 (2006)
20. N. Zhang, A. Anpalagan, Telecommunication Systems **44**, 17 (2010)
21. J.S. Baras, S. Perumal, V. Tabatabaee, K. Somasundaram, P. Purkayastha, in *Proc. WICON '08* (2008)
22. R. Urgaonkar, V. Manfredi, R. Ramanathan, in *IEEE Communication Systems and Networks (COMSNETS)* (2013)
23. R. Ramanathan, A. Samanta, T.L. Porta, in *Proc. of the 9th ACM PE-WASUN* (ACM, 2012), pp. 31–38
24. S. Hanly, D. Tse, Information Theory, IEEE Transactions on **44**(7), 2816 (1998)
25. R. Urgaonkar, M. Neely, Information Theory, IEEE Transactions on **60**(3), 1869 (2014)
26. Y. Shi, Y.T. Hou, J. Liu, S. Kompella, IEEE Trans. Mob. Comput. **12**(7), 1404 (2013)
27. S. Ramanathan, Wirel. Netw. **5**, 81 (1999)
28. C. Young, in *Proc. IEEE MILCOM* (1996)
29. D. Vassis, G. Kormentzas, A. Rouskas, I. Maglogiannis, Network, IEEE **19**(3), 21 (2005)
30. J. Redi, R. Ramanathan, in *MILITARY COMMUNICATIONS CONFERENCE, 2011 - MILCOM 2011* (2011), pp. 2258 –2263
31. N. Gupta, P. Kumar, COMMUNICATIONS IN INFORMATION AND SYSTEMS **3** (2004)
32. Q. Chen, F. Schmidt-Eisenlohr, D. Jiang, M. Torrent-Moreno, L. Delgrossi, H. Hartenstein, in *Proceedings of MSWiM '07* (2007), pp. 159–168
33. M. Gast, *802.11 Wireless Networks: A Definitive Guide* (O'Reilly Publications, 2005)
34. S.R. Y. Zhang, G. Cao, T.F.L. Porta, P. Basu, in *MILCOM 2011* (Baltimore, 2011)
35. P. Hilton, J. Pedersen, The Mathematical Intelligencer **13**, 64
36. T. Cormen, C. Leiserson, R. Rivest, *Introduction to algorithms* (MIT Press McGraw-Hill, Cambridge, Mass., 1990)